

Sensorless Contact Position Estimation of a Mobile Robot in Pushing Motion

HA.ND. Dayarathna, L.L.G. Prabuddha, K.L.D.N.J Ariyawansa, M.K.C.D. Chinthaka,
 A.M. Harsha S. Abeykoon, M. Branesh Pillai Department of Electrical
 Engineering, University of Moratuwa
 Katubedda, Sri Lanka
 nishaldd@gmail.com, gayaann@gmail.com, darshanikl@gmail.com, dineshchinthakal@gmail.com,
 harsha@elect.mrt.ac.lk, pillaiبرانesh@elect.mrt.ac.lk,

Abstract- Manipulating mobile robots on a pre-defined path is a challenging task when there are unknown objects on its path. Most of the manipulators use gripping methods to move such obstacles. In this research, an object to be pushed in a predefined path is considered. Estimation of the point of contact is important to control the mobile robot in its desired path. This paper introduces a novel concept called Contact Position Estimator (CPE) to calculate the point of contact when the robot is moving on the said path. CPE estimates the position using the reaction torque observer and the estimated torque, which is a sensorless method of estimating the torque, was used. Results show the applicability of the proposed concept.

Key words: Contact Position Estimator, Disturbance Observer, Reaction Torque Observer, Wheeled Mobile Robot.

I. INTRODUCTION

Moving an object from one position to another is one of the basic tasks of a robot. Normally most of the robot manipulators could grip the object, pick it up and place it at the desired position. But when the object is too large, too heavy or complex to be gripped, pushing could play a great roll in these complex tasks. This paper focuses on a pushing task that a mobile robot pushes an object and so that it can follow a given path without sliding it away. Pushing is used to change both the position and the orientation of the objects. However pushing has several advantages over gripping the objects. It allows for easier simultaneous manipulation of groups of the objects, permits the manipulation of larger and heavier objects, and most importantly requires a simpler and cheaper robot structure than in gripping. However the pushing motion has some drawbacks. When an object is being pushed it may easily move away from the pushing manipulator. Pushing is also mechanically unstable, and thus various control problems arise. If the object is pushed away the navigating robot should frequently reverse and bring the object to its 'middle region' of contact. Consequently, the successful completion of a pushing manipulation task requires planning.

Therefore for successful pushing operation for an object in a pre-defined path requires a correct estimation of the point of contact. The main objective of this research is to detect the point of contact without the use of any torque/force sensors in an any given path. This method could be used specially in factories where objects could be pushed for a shorter distances from point to point. In this paper a flat terrain is considered.

Reaction Torque Observer (RTOB) which is a variant of Disturbance Observer (DOB) [1] is used to estimate the external torque.

II. MODELLING

It is assumed that the mobile robot's inertia is sufficiently larger than the object being pushed such that no wheels slipping is there.

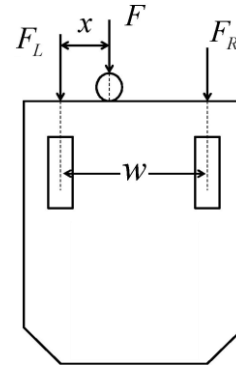


Fig. 1. Components of the Reaction Force

If the mobile robot is met an obstacle, there will be additional torques on two wheels. Assume the point of contact is "x" distance away from the left hand side wheel as shown in Fig. 1.

Assume the force exerted on the manipulator is F at the point of contact. This external force can be divided in to two components exerted on the two wheels as FL and FR. These two forces can be calculated by taking the fractional components of F assuming that the distance of the two wheels of the manipulator is "w".

$$F_L = \frac{F(w-x)}{w} \text{ and } F_R = \frac{Fx}{w} \quad (1)$$

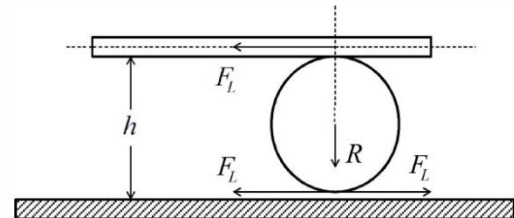


Fig. 2. Components of the FL in the left wheel's plane.

These two forces can again be decomposed into the plane parallel to the forces F_L and F_R to convert it to the torques acting on the wheels. It is shown in the Fig. 2.

$$T_L = (F_L \cdot h - F_L \cdot R) = F_L(h - R) \quad (2)$$

Similarly,

$$\tau_R = (F_R \cdot H - F_R \cdot R) = F_R(h - R) \quad (3)$$

By using equations (1),

$$\tau_L = \frac{F(w-x)}{w}(h - R) \quad (4)$$

$$\tau_R = \frac{Fx}{w}(h - R) \quad (5)$$

Using the equations (4) and (5), following equation can be derived as;

$$\frac{\tau_L}{\tau_R} = \frac{(w-x)}{w} \quad (6)$$

Rearranging the equation (6),

$$x = \frac{\tau_R w}{(\tau_L + \tau_R)} \quad (7)$$

III. DISTURBANCE OBSERVER (DOB) AND REACTION TORQUE OBSERVER (RTOB)

A. Disturbance Observer (DOB)

Robotic manipulators are often subjected to different types of unknown disturbances such as external loads. If such disturbances are not accounted for calculations, the performance of the robot may tend to degrade and may even cause the instability of control system. Controlling a mobile robot with unknown disturbances is a challenging problem. Disturbance observer is used to suppress unwanted disturbances from the system [2]. This estimation may then be used to compensate for the disturbance torque acting on the shaft thus improving the system's robustness to external torques and load changes. The magnitude of the disturbance can be estimated and then be used to improve the performance of manipulator.

The disturbance torque can be obtained from equation (8) [3]. Here, K_t is the motor constant of the motor, J_n is the inertia of the load coupled to the rotor, the subscript n is used to denote the nominal values.

$$T_{dis} = K_{tn} I_a^{ref} - J_n \ddot{\theta} \quad (8)$$

After transferring the above equation in to a control diagram is shown in Fig.3.

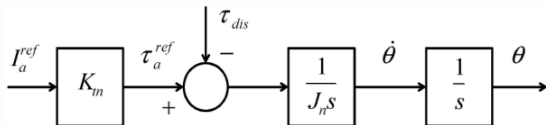


Fig.3. Control diagram of the motor with the disturbance torque.

Therefore the disturbance torque (τ_{dis}) can be calculated from angular acceleration of the motor and the current reference. In practical situations, the angular acceleration cannot be measured directly using available sensors. So, it is normally calculated by differentiating the angular displacement measured from the wheel encoders.

As shown in Fig. 4, τ_l is the external load torque, $f + D\dot{\theta}$ represents the sum of the fixed friction and viscous friction, $\hat{\tau}_{dis}$ is the estimated disturbance torque, I_a is the reference current for the acceleration. Furthermore, a low pass filter should be used at the output of the disturbance torque calculation because of the differentiator used in estimating the acceleration. If the used filter is of the first order, the output can be expressed as,

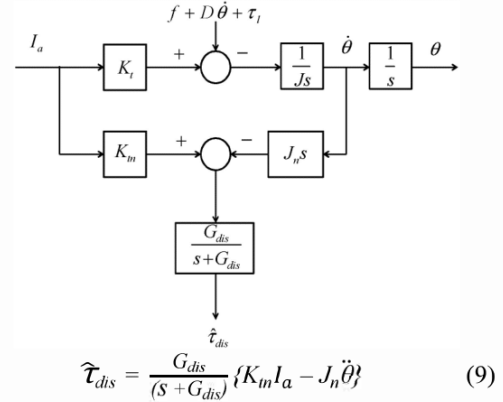


Fig.4. Block diagram of the disturbance observer

Here (G_{dis}) is the angular cutoff frequency of the low pass filter. The disturbance observer estimates the disturbance torque on the control system and compensates for it.

B. Reaction Torque Observer (RTOB)

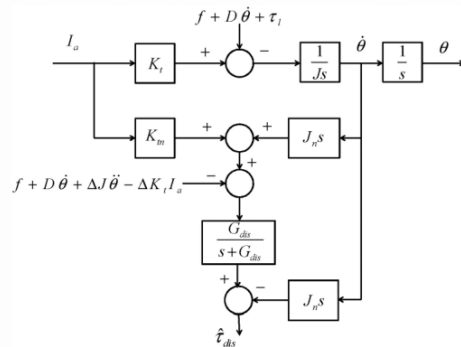


Fig.5. Block diagram of the reaction torque observer

When the mobile robot is moving in a curved path the torques applied on two wheels will be different even without any disturbance. Therefore, it is important to estimate only the torque applied to the mobile robot due to the object being pushed. For that, reaction torque observer used to calculate only the external forces [4].

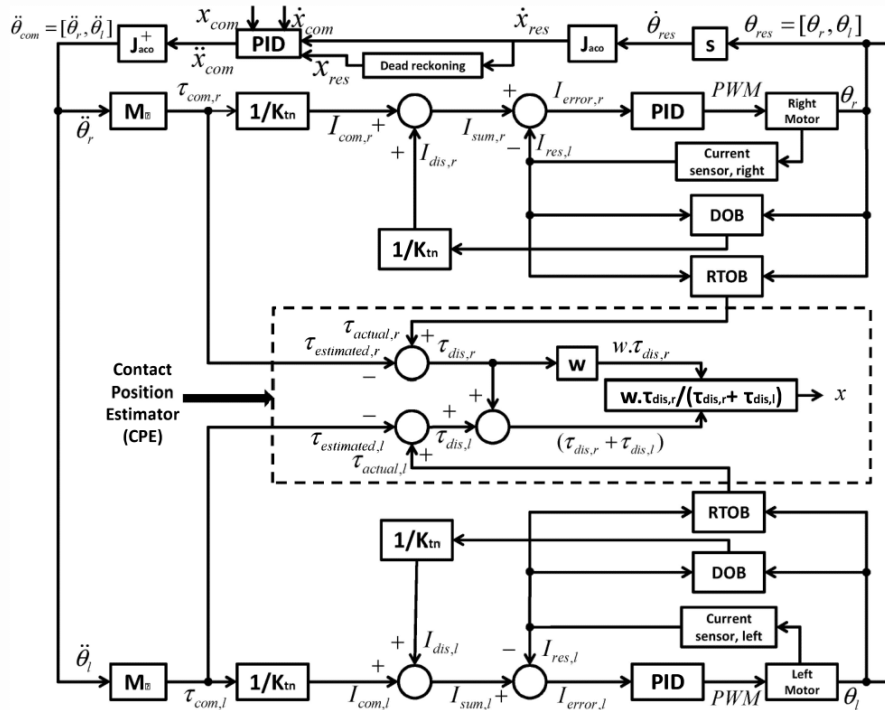


Fig. 6. Block diagram of Contact Position Estimator

IV. CONTACT POSITION ESTIMATOR (CPE)

Consider that the robot is manipulated on a pre-defined path as shown in Fig. 7.

CPE is designed to estimate the point of contact of the object on the robot. The inputs to the CPE are the estimated torque and the actual torque of the two motors separately at the instant of contact.

When the mobile robot is manipulated on a curved path the torques applied on two wheels will be different even without any disturbances. This is because the wheels of the mobile robot are having different velocities to follow the pre-defined path. Thus, the disturbance observer alone may mistakenly identify this as a disturbance torque. Therefore, ‘reaction torque observer (RTOB)’ is introduced to overcome this problem.

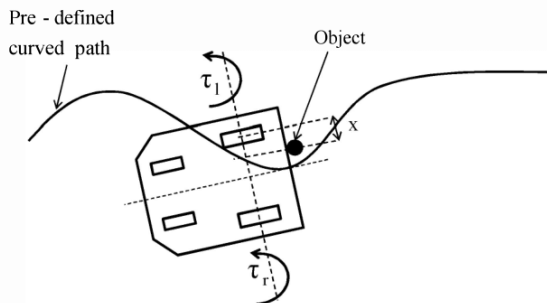


Fig.7. Robot is manipulated on a pre-defined path

The actual torque of the motors can be obtained from the output of the RTOB and the estimated torque profile of the motors can be calculated for the path which the robot is being manipulated. Then the disturbance torque can be obtained by using the difference between the actual and estimated values of torques on the wheels. The complete block diagram for this process is shown in Fig. 6.

This method can be applied for paths having constant or variable radii. Load torques on the two wheels will be different in both the above scenarios even without causing a disturbance. When the robot manipulator is being operated on a non-straight path, left and right wheel motors are expected to produce time varying different torques according to the path it follows. Therefore, the instantaneous values of the estimated load torques have to be considered when calculating the point of contact of the object.

V. KINEMATICS OF THE WHEELED MOBILE ROBOT (WMR)

The velocity and displacement instructions to the WMR were given with respect to a world coordinate system. Therefore, the angular velocities and displacements of the driven wheels should be converted to the world coordinate system data. This is done using the following kinematic model [5].

As shown in Fig.8 the position of the robot (P_o) which is the middle point of the line connecting the axis of two wheels is defined using the world coordinate system. It consists of, X coordinate(x) which is the distance the robot platform has travelled in X direction, the Y coordinate(y) which is the

distance the robot platform has travelled in Y direction and the attitude angle (ϕ) which is the angle formed between the perpendicular to the mobile robot's axis and the x axis.

Therefore, if the angle of rotation of left and right wheels (θ_l, θ_r , respectively) and the pose vector of robot platform in the surface is described in equations (10) and (11).

$$\theta = [\theta_l, \theta_r]^T \quad (10)$$

$$X = [x, y, \phi]^T \quad (11)$$

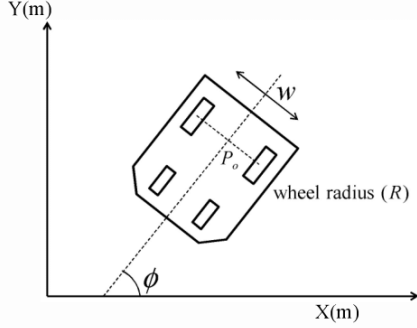


Fig. 8. The kinematics model in world coordinate system

Then the direct kinematic equation can be represented in equation (12),

$$\dot{X} = J_{aco} \cdot \dot{\theta} \quad (12)$$

Where J_{aco} represent the Jacobean matrix calculated as given in equation (13),

$$J_{aco} = \begin{bmatrix} \frac{R \cdot \cos \phi}{2} & \frac{R \cdot \cos \phi}{2} \\ \frac{R \cdot \sin \phi}{2} & \frac{R \cdot \sin \phi}{2} \\ \frac{R}{W} & \frac{-R}{W} \end{bmatrix} \quad (13)$$

However, it is required to calculate the inverse kinematic equation in order to plan the robot motion and the robot control. Since Jacobean matrix is not a quadratic matrix, the pseudo inverse matrix J_{aco}^+ has to be used. The kinematic equation has to be differentiated to calculate the inverse kinematic equations.

$$\dot{\theta} = J_{aco}^+(\phi) \cdot \dot{X} \quad (14)$$

$$\ddot{\theta} = J_{aco}^+(\phi) \cdot \ddot{X} + \dot{J}_{aco}^+(\phi) \cdot \dot{X} \quad (15)$$

Where J_{aco}^+ represents the inverse Jacobean matrix,

$$J_{aco}^+ = \frac{1}{R} \begin{bmatrix} \cos \phi & \sin \phi & \frac{W}{2} \\ \cos \phi & \sin \phi & \frac{-W}{2} \end{bmatrix} \quad (16)$$

By neglecting the inverse Jacobean derivative,

$$\ddot{\theta} = J_{aco}^+(\phi) \cdot \ddot{X} \quad (17)$$

A. Dead – Reckoning

WMR can estimate the current position and attitude angle by using dead reckoning. For that, the velocity, angular displacement feedbacks and the previously calculated position and attitude angle data are used [6].

Estimated values of x and y positions are found as follows.

$$X_k = X_{k-1} + v_{p,k} \cdot \cos\left(\frac{\phi_k + \phi_{k-1}}{2}\right) \cdot \Delta t \quad (18)$$

$$y_k = y_{k-1} + v_{p,k} \cdot \sin\left(\frac{\phi_k + \phi_{k-1}}{2}\right) \cdot \Delta t \quad (19)$$

Where, V_p is the velocity of the WMR in world coordinate system and Δt is the sampling time. The subscript k used to indicate their respective values at K^{th} sampling moment and the subscript $k - 1$ denotes the values at the pervious occasion of sampling.

The attitude angle can be calculated from the encoder output from the equation (20),

$$\phi = \frac{R}{W} \cdot (\theta_r - \theta_l) \quad (20)$$

VI. DYNAMICS OF THE WMR

The motion of a WMR is related to the forces or torques the system is subjected to. Dynamic analysis of WMR is important due to the problem of the control of the system, which is in contact with its environment. Dynamics of the mobile robot can be described as follows.

It is assumed that, the Centre of Gravity (COG) of the mobile robot is located at bisect of the driven wheel axis. The forward movement of the WMR is produced by the traction force. When a wheel is rolling on a ground surface, the shear force is generated at the wheel and the ground contact point and it corresponds to the traction force. This force depends on the magnitude of the longitudinal force. For this analysis assume an ideal case where there is no slip on the wheels. This condition happens when the contact point between the wheel and the ground surface is assumed to be instantaneously stationary, and the resultant traction force is treated as a static friction [7]. Furthermore, the forces applied on the WMR due to the viscous friction are neglected.

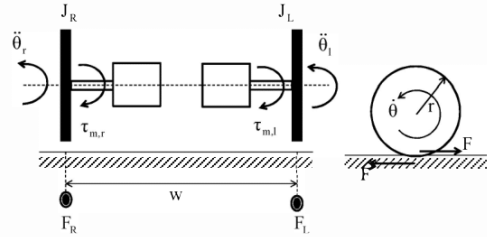


Fig. 9. Generation of traction force for mobility of the WMR

Let, mass of the robot platform to be M , the inertia of the robot platform around an axis vertical to the $x - y$ plane J and inertia of left and right wheels be J_l and J_r respectively.

Therefore for the WMR, the dynamic equations of right and left wheel are expressed as,

$$\tau_{m,r} - r.F_r = J_r.\ddot{\theta}_r \quad (21)$$

$$\tau_{m,l} - r.F_l = J_l.\ddot{\theta}_l \quad (22)$$

Since, there is no slip conditions the WMR cannot have longitudinal movement and it is considered that the WMR at a given moment is travelling in circle of radius R as shown in Fig.10.

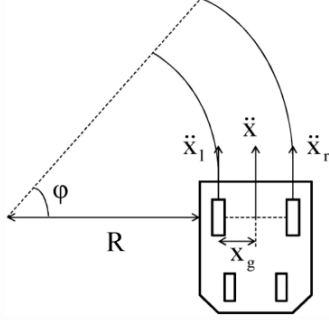


Fig.10. Motion of the WMR due to the non-holonomic restriction

$$\ddot{x}_l = R.\ddot{\phi} = r.\ddot{\theta}_l \quad (23)$$

$$\ddot{x}_r = (R+W).\ddot{\phi} = r.\ddot{\theta}_r \quad (24)$$

If the linear acceleration of the centre of gravity of the platform is denoted by \ddot{x} ,

$$F_r + F_l = M.\ddot{x} \quad (25)$$

$$\ddot{x} = (R+x_g).\ddot{\phi} \quad (26)$$

Where x_g is the distance to the centre of gravity from the left wheel along the driving wheel axis.

Assume that,

$$x_g = w/2 \quad (27)$$

Equation (28) can be derived from equations (23), (24), (25), (26) and (27).

$$\ddot{X} = \frac{r}{2}(\ddot{\theta}_r + \ddot{\theta}_l) \quad (28)$$

Also,
$$R = \frac{w.\ddot{\theta}_l}{\ddot{\theta}_r - \ddot{\theta}_l} \quad (29)$$

$$\alpha = \ddot{\phi} = \frac{r}{w}(\ddot{\theta}_r - \ddot{\theta}_l) \quad (30)$$

In the Newtonian reference frame, for the motion of the WMR,

$$\tau = I.\alpha \quad (31)$$

$$F_r(w + R) + F_l.R = \{J + M.(x_g + R)^2\}.\alpha \quad (32)$$

Therefore from equations (25) and (32),

$$F_r = \frac{1}{w} \{ \alpha (J + M.(x_g + R)^2) - M.R.\ddot{x} \} \quad (33)$$

By substituting F_r from equation (33) to equation (21),

$$\tau_{m,r} = \frac{r}{w} \{ \alpha (J + M.(x_g + R)^2) - M.R.\ddot{x} \} + J_r.\ddot{\theta}_r \quad (34)$$

By substituting \ddot{x} , R and $\frac{r}{w}$ from equations (28), (29), (30) in to equation (34),

$$\tau_{m,r} = r^2 \left[\left\{ \frac{J}{w^2} + \frac{M}{4} + \frac{J_r}{r^2} \right\} \ddot{\theta}_r + \left\{ \frac{M}{4} - \frac{J}{w^2} \right\} \ddot{\theta}_l \right] \quad (35)$$

Also considering (22) we can arrive at,

$$\tau_{m,l} = r^2 \left[\left\{ \frac{J}{w^2} + \frac{M}{4} + \frac{J_l}{r^2} \right\} \ddot{\theta}_l + \left\{ \frac{M}{4} - \frac{J}{w^2} \right\} \ddot{\theta}_r \right] \quad (36)$$

By equating equations (35) and (36), we can relate the torque requirements of the right and left motors with respect to their angular acceleration.

The torque requirements of the right and left wheels can be expressed in vector form in the following manner,

$$\tau = [\tau_{m,r}, \tau_{m,l}]^T \quad (37)$$

Also the angular accelerations of the driving wheels, can also be combined in a vector as,

$$\ddot{\theta} = [\ddot{\theta}_r, \ddot{\theta}_l]^T \quad (38)$$

Then the relationship between the torque requirement and the angular acceleration of the driving wheels can be expressed by the vector equation,

$$\tau = M_\theta.r^2.\ddot{\theta} \quad (39)$$

Where,

$$M_\theta = \begin{bmatrix} \left\{ \frac{J}{w^2} + \frac{M}{4} + \frac{J_r}{r^2} \right\} & \left\{ \frac{M}{4} - \frac{J}{w^2} \right\} \\ \left\{ \frac{M}{4} - \frac{J}{w^2} \right\} & \left\{ \frac{J}{w^2} + \frac{M}{4} + \frac{J_l}{r^2} \right\} \end{bmatrix} \quad (40)$$

This relationship constitutes the dynamic model of the WMR represented by the matrix form and it is called the inertia matrix.

VII. RESULTS

For this research two wheeled mobile robot is used. Two rotary encoders are connected to the wheels which are attached to two DC motors, there are two current sensors connected to the two DC motors. The robot is shown in Fig 11. Mobile robot is controlled by an MBED LPC 1768 microcontroller of 96MHz.

Mobile robot is manipulated on a pre-defined path, without pushing an object. Mobile robot is given a constant acceleration input. This scenario is equivalent to a case where the robot is pushing an object by its mid-point. Since CPE is

calculating the distance from the right motor, the output of the CPE for this scenario should be 0.1875m. Disturbance torques of the two motors and the output of the CPE for this scenario are shown in Fig. 12 and Fig. 13 respectively.

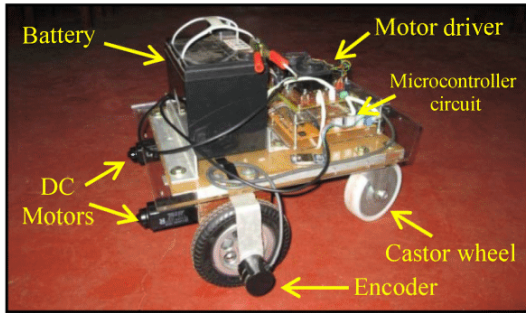


Fig. 11. Mobile robot used for the research

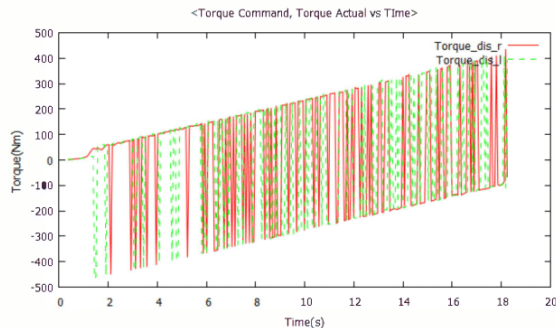


Fig. 12. Torques of the motors without disturbance

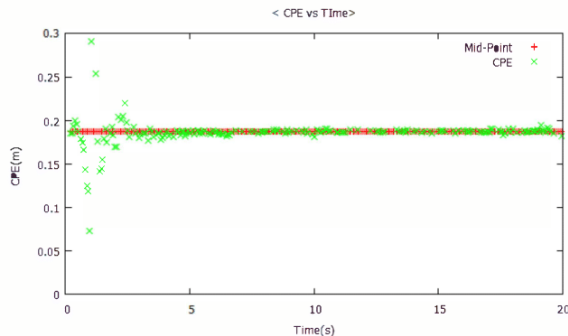


Fig. 13. CPE without disturbance

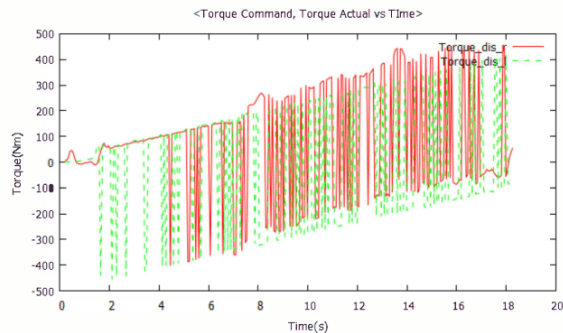


Fig. 14. Torques of the motors with disturbance

Since the starting torques of the two motors are different, the output of the CPE deviates from the desired value initially. However from Fig.12 it is evident, that the torques of the left

and right wheels coincides as expected. Estimated CPE shows correct values after the initial transient.

In the next scenario the robot is manipulated while pushing an object in a distance of 0.16m from the right motor. Disturbance torques of the two motors and the output of CPE for this scenario are shown in Fig. 14 and Fig. 15. As for the results, it is evident that the CPE has estimated the contact position to a 90% accuracy.

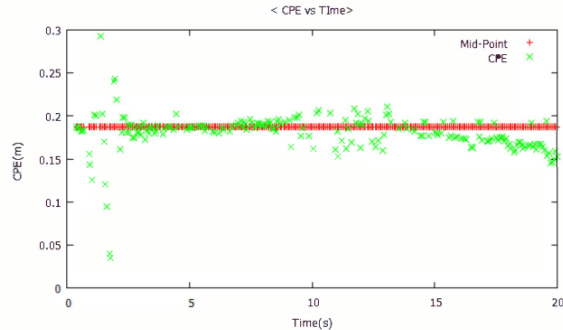


Fig. 15. CPE with disturbance

VIII. CONCLUSIONS

In this paper we propose a novel concept to estimate the position of contact when the robot is in pushing motion. The validity of the concept is verified experimentally. Hence the contact position of an object on a mobile robot can be calculated without using additional sensors. However the accuracy of the CPE could be further enhanced by fine tuning the disturbance observer and the reaction torque observer.

IX. ACKNOWLEDGEMENTS

Authors would like to express their gratitude to MBED (mbed.org) for providing microcontrollers for this research.

X. REFERENCES

- [1] T.Murakami, F. YU, K.Ohnishi: "Torque sensorless control in multidegree-of-freedom manipulator," *Industrial Electronics, IEEE Transaction on*, vol.40,no.2,pp.259-265, Apr-1993.
- [2] K.Ohnishi, N. Matsui, Y.Hori, "Estimation Identification, and Sensorless Control in Motion Control System," *Proceedings of the IEEE*, Vol. 82, No.8, pp 1253-1265, August 1994.
- [3] Hasala R. Senevirathne, A.M.Harsha S.Abeykoon, M. Branesh Pillai: "Disturbance Rejection Analysis of a Disturbance Observer based Velocity Controller," *ICIA'S'12, Proceeding of the 6th IEEE Conference*, Sep 27-29, 2012
- [4] Mizuochi, M.; Tsuji, T.; Ohnishi, K.; , "Improvement of disturbance suppression based on disturbance observer," *Advanced Motion Control, 2006. 9th IEEE International Workshop on*, vol.,no., pp.229-234, 0-0 0.
- [5] Abeykoon, A.M.H.S.; Ohnishi, K.; , "Traction force improvement of a two wheel mobile manipulator by changing the centre of gravity," *Industrial Informatics, 2005. INDIN '05. 2005 3rd IEEE International Conference on*, vol., no., pp. 756- 760, 10-12 Aug. 2005.
- [6] S. Katsura, K. Ohnishi, and K. Ohishi, "Transmission of force sensation by environment quarryer based on multilateral control," *IEEE Tran. Ind. Electron.*, vol. 54, no2, pp. 898-906, Apr.2007.
- [7] Sidek, N.; Sarkar, N.;"Dynamic Modeling and Control of Nonholonomic Mobile Robot with Lateral Slip," *Systems, 2008. ICONS 08. Third International Conference on*, vol., no., pp.35-40, 13-18 April 2008.